

# Synthesis, Spectroscopic, and Substituent-Dependent Self-Assembling Structural Characterization of Ferrocenyl-Containing Silanediols, $\text{Fc(R)Si(OH)}_2$ , $\text{R} = \text{Me, CH}_2=\text{CHCH}_2, n\text{-Bu, } t\text{-Bu, Ph, } c\text{-Hx}$ , Including Transformation to a Ferrocenyl Stannasiloxane, $[\text{OSiFc}(n\text{-Bu})\text{O}(t\text{-Bu})_2\text{Sn}]_2$

Enrique A. Reyes-García, Francisco Cervantes-Lee, and Keith H. Pannell\*

Department of Chemistry, University of Texas at El Paso, El Paso, Texas 79968-0513

Received May 8, 2001

The hydrolysis of ferrocenyldichlorosilanes,  $\text{Fc(R)SiCl}_2$ ,  $\text{Fc} = (\eta^5\text{-C}_5\text{H}_5)\text{Fe}(\eta^5\text{-C}_5\text{H}_4)$ ,  $\text{R} = \text{methyl (Me), } \mathbf{1a}$ ; 2-propenyl (allyl),  $\mathbf{1b}$ ;  $n$ -butyl ( $n\text{-Bu}$ ),  $\mathbf{1c}$ ;  $tert$ -butyl ( $t\text{-Bu}$ ),  $\mathbf{1d}$ ; phenyl (Ph),  $\mathbf{1e}$ ; cyclohexyl ( $c\text{-Hex}$ ),  $\mathbf{1f}$ , leads to the formation of new ferrocenylsilanediols,  $\text{Fc(R)Si(OH)}_2$ ,  $\mathbf{2a-f}$ . The diols have been characterized by  $^1\text{H}$ ,  $^{13}\text{C}$ , and  $^{29}\text{Si}$  NMR, IR, UV/vis, and elemental analysis and in the case of  $\mathbf{2d}$  and  $\mathbf{2f}$  by single-crystal X-ray diffraction. The latter two compounds reveal a primary double-chain structure of silanediols achieved via intermolecular hydrogen bonding, with further hydrogen bonding resulting in ladder structures. The reactivity of  $\text{Fc}(n\text{-Bu})\text{Si(OH)}_2$  was probed by its reaction with di- $tert$ -butyldichlorostannane to form the distannadisiloxane  $[\text{OSiFc}(n\text{-Bu})\text{OSn}(t\text{-Bu})_2]_2$ , whose single-crystal structure was shown to be that of the *cis* isomer, which in solution formed a mixture of the *cis* and *trans* isomers.

## Introduction

The synthesis of organosilicon materials containing transition metals,<sup>1</sup> and more recently those containing ferrocenyl and ferrocenylene units,<sup>2</sup> has been the center of extensive investigations. In the case of ferrocenyl derivatives such activity is driven by the reversible redox behavior, permeability, and thermal and photochemical stability that this group can impart to molecular systems, such as polymers,<sup>3</sup> catalyst precursors,<sup>4</sup>

and dendrimers.<sup>5</sup> In addition to a series of ferrocene-containing siloxane and metallasiloxane silanols,<sup>6</sup> ferrocene-containing disiloxanediols and silanediols have been reported,<sup>6,7</sup> of particular interest since silanediols and silanetriols crystallize in the solid state into su-

(1) Brook, M. A. *Silicon in Organic, Organometallic, and Polymer Chemistry*; Wiley-Interscience: New York, 2000; Chapter 6. (b) Eisen, M. S. In *The Chemistry of Organic Silicon Compounds*; Rappoport, Z., Apeloig, Y., Eds.; Wiley-Interscience: New York, 1998; Vol. 2, Chapter 35. (c) Jutzi, P. In *The Chemistry of Organic Silicon Compounds*; Rappoport, Z., Apeloig, Y., Eds.; Wiley: New York, 1998; Vol. 2, Chapter 36.

(2) (a) Dement'ev, V. V.; Cervantes-Lee, F.; Parkanyi, L.; Sharma, H.; Pannell, K. H. *Organometallics* **1993**, *12*, 1983. (b) Pannell, K. H.; Dement'ev, V. V.; Li, H.; Cervantes-Lee, F.; Nguyen, M. T.; Diaz, A. F. *Organometallics* **1994**, *13*, 3644. (c) Sharma, H.; Vincenti, S. P.; Vicari, R.; Cervantes-Lee, F.; Pannell, K. H. *Organometallics* **1990**, *9*, 2109. (d) Pannell, K. H.; Wang, F.; Sharma, H.; Cervantes-Lee, F. *Polyhedron* **2000**, *19*, 291. (e) Sharma, H.; Pannell, K. H.; Ledoux, I.; Zyss, J.; Ceccanti, A.; Zanello, P. *Organometallics* **2000**, *19*, 770.

(3) (a) Zeigler, J. M.; Fearon, F. W. G., Eds. *Silicon Based Polymer Science: A Comprehensive Resource*. Advances in Chemistry Series No. 224; American Chemical Society: Washington D.C., 1990. (b) Kapoor, R. N.; Crawford, G. M.; Mahmoud, J.; Dement'ev, V. V.; Nguyen, M. T.; Diaz, A. F.; Pannell, K. H. *Organometallics* **1995**, *14*, 4944. (c) MacLachlan, M. J.; Lough, A. J.; Geiger, W. E.; Manners, I. *Organometallics* **1998**, *17*, 1873. (d) Nguyen, P.; Stojcevic, G.; Kulbaba, K.; MacLachlan, M.; Liu, X.; Lough, A. J.; Manners, I. A. *Macromolecules* **1998**, *31*, 5983. (e) Gomez-Elipe, P.; MacDonald, P. M.; Manners, I. *Angew. Chem., Int. Ed. Engl.* **1997**, *36*, 762. (f) Nguyen, P.; Gomez-Elipe, P.; Manners, I. *Chem. Rev.* **1999**, *99*, 1515. (g) MacLachlan, M.; Ginzburg, M.; Coombs, N.; Raju, N. P.; Greedan, J. E.; Ozin, G. A.; Manners, I. *J. Am. Chem. Soc.* **2000**, *122*, 3878. (h) Power-Billard, K. N.; Manners, I. *Macromolecules* **2000**, *33*, 26.

(4) Togni, A.; Hayashi, T. *Ferrocenes: homogeneous catalysis, organic synthesis, materials science*; VCH: New York, 1995.

(5) (a) Newkome, G. R.; Moorefield, C. N.; Vogtle, F. *Dendritic Molecules: Concepts, Synthesis, and Perspectives*; VCH: Weinheim, Germany, 1996. (b) Cardona, C. M.; Kaifer, A. E. *J. Am. Chem. Soc.* **1998**, *120*, 4023. (c) Cuadrado, I.; Casado, C. M.; Alonso, B.; Morán, M.; Losada, J.; Belsky, V. *J. Am. Chem. Soc.* **1997**, *119*, 7613. (d) Valério, C.; Fillaut, J.; Ruiz, J.; Guittard, J.; Blais, J.; Astruc, D. *J. Am. Chem. Soc.* **1997**, *119*, 2588.

(6) (a) Casado, C. M.; Moran, M.; Losada, J.; Cuadrado, I. *Organometallics* **1993**, *12*, 4327. (b) Casado, C. M.; Moran, M.; Losada, J.; Cuadrado, I. *Inorg. Chem.* **1995**, *34*, 1668. (c) Gomez-Elipe, P.; MacDonald, P. M.; Manners, I. *Angew. Chem., Int. Ed. Engl.* **1997**, *36*, 762. (d) Wang, J.; Collinson, M. M. *J. Electroanal. Chem.* **1998**, *455*, 127. (e) Cerveau, G.; Corriu, R. J. P.; Costa, N. *J. Non-Cryst. Solids* **1993**, *163*, 235.

(7) (a) MacLachlan, M. J.; Ginzburg, M.; Zheng, J.; Knoll, O.; Lough, A. J.; Manners, I. *New J. Chem.* **1998**, *22*, 1409. (b) MacLachlan, M. J.; Zheng, J.; Lough, A. J.; Manners, I. *Organometallics* **1999**, *18*, 1337. (c) MacLachlan, M. J.; Zheng, J.; Thieme, K.; Lough, A. J.; Manners, I.; Mordas, C.; LeSuer, R.; Geiger, W. E.; Liable-Sands, L. M.; Rheingold, A. L. *Polyhedron* **2000**, *19*, 275.

(8) Lickiss, P. D. *Adv. Inorg. Chem.* **1995**, *42*, 146, and references therein.

(9) (a) King L.; Sullivan A. *Coord. Chem. Rev.* **1999**, *189*, 19. (b) Beckmann, J.; Jurkschat, K.; Schürmann, M. *J. Organomet. Chem.* **2000**, *602*, 170. (c) Voigt, A.; Murugavel, R.; Roesky, H. W. *Organometallics* **1996**, *15*, 5097. (d) Beckmann, J.; Jurkschat, K.; Pieper, N.; Schürmann, M. *Chem. Commun.* **1999**, *12*, 1045. (e) Beckmann, J.; Jurkschat, K.; Müller, D.; Rabe, S.; Schürmann, M. *Organometallics* **1999**, *18*, 2326. (f) Beckmann, J.; Jurkschat, K.; Rabe, S.; Schürmann, M.; Dakternieks, D.; Duthie, A. *Organometallics* **2000**, *19*, 3272. (g) Beckmann, J.; Biesemans, M.; Hassler, K.; Jurkschat, K.; Martins, J. C.; Schürmann, M.; Willem, R. *Inorg. Chem.* **1998**, *37*, 4891. (h) Beckmann, J.; Jurkschat, K.; Schollmeyer, D.; Schürmann, M. *J. Organomet. Chem.* **1997**, *543*, 229. (i) Mehring, M.; Schürmann, M.; Jurkschat, K. *Organometallics* **1998**, *17*, 1227. (j) Cervantes-Lee, F.; Sharma, H.; Haiduc, I.; Pannell, K. H. *J. Chem. Soc., Dalton Trans.* **1998**, *1*.

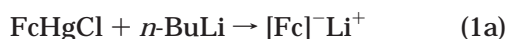
pramolecular arrays.<sup>8</sup> Although a range of metallasiloxanes M–O–Si, M = Si, Ge, Sn, B, are known,<sup>9</sup> few systems that incorporate electrochemically active molecules such as ferrocene have been explored.

We report the synthesis of new ferrocenylsilanediol materials containing a number of organic substituents, Fc(R)Si(OH)<sub>2</sub>, Fc = (η<sup>5</sup>-C<sub>5</sub>H<sub>5</sub>)Fe(η<sup>5</sup>-C<sub>5</sub>H<sub>4</sub>), R = methyl (Me), **2a**; 2-propenyl (allyl), **2b**; *n*-butyl (*n*-Bu), **2c**; *tert*-butyl (*t*-Bu), **2d**; phenyl (Ph), **2e**; cyclohexyl (*c*-Hex), **2f**, formed by the hydrolysis of the corresponding ferrocenylsilanediol dichlorides, Fc(R)Si(Cl)<sub>2</sub>, **1a–f**. Along with their spectroscopic characterization, we report the single X-ray diffraction analysis of Fc(*t*-Bu)Si(OH)<sub>2</sub> and Fc(*c*-Hex)Si(OH)<sub>2</sub>, and that of the stannasiloxane [OSiFc(*n*-Bu)OSn(*t*-Bu)<sub>2</sub>]<sub>2</sub> derived from the reaction of **2c** with (*t*-Bu)<sub>2</sub>SnCl<sub>2</sub>.

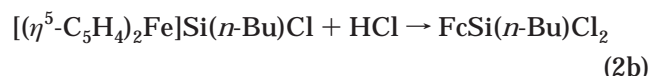
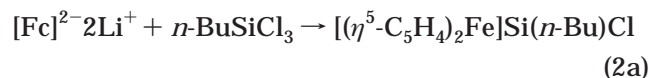
## Results and Discussion

### Synthesis and Spectra of Fc(R)SiX<sub>2</sub>, X = Cl, OH.

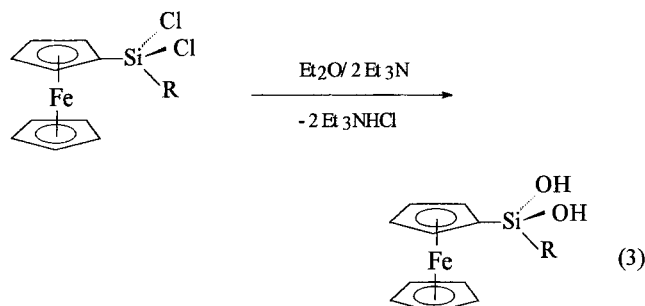
All except one of the dichloro compounds were prepared by the direct salt-elimination sequence outlined in eq 1, R = Me, **1a**; allyl, **1b**; *t*-Bu, **1d**; Ph, **1e**; *c*-Hex, **1f**.



Ferrocenyldichloro(*n*-butyl)silane, **1c**, was prepared by the HCl treatment of the [1]-(chloro(*n*-butyl)silylene)-ferrocenophane, eq 2.



The <sup>1</sup>H, <sup>13</sup>C, and <sup>29</sup>Si NMR spectra of compounds **1a–f** are fully consistent with their proposed structures and related literature data for ferrocenyl-substituted chlorosilanes.<sup>10,11</sup> Hydrolysis of **1a–f** was performed according to published procedures for the preparation of organosilanols, eq 3.<sup>12–14</sup>



In all cases the resulting diols were yellow solids obtained in moderately high (78%) to low (12%) yields. Ferrocenyl(methyl)silanediol was the most insoluble of the compounds synthesized; consequently its NMR spectrum was acquired in DMSO-*d*<sub>6</sub> in which a single sharp resonance at 5.98 ppm indicated the presence of a strongly solvent-hydrogen-bonded silanediol. The <sup>1</sup>H NMR spectra of the other silanediols were obtained in CDCl<sub>3</sub> and exhibited the typical broad resonance be-

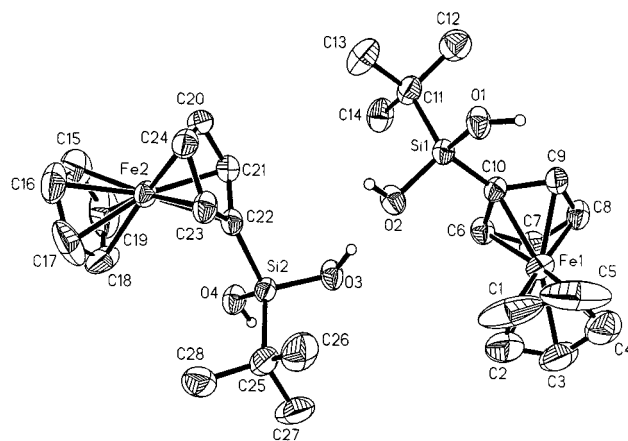


**Figure 1.** (a) Structure and atom-numbering scheme of Fc(*t*-Bu)Si(OH)<sub>2</sub>; thermal ellipsoids at 50% probability level.

tween 2 and 4 ppm for exchanging OH protons. The characteristic sharp SiO–H stretching frequencies of silanols, centered approximately at 3680–3640 cm<sup>-1</sup>, were observed together with the corresponding broad H-bonded frequency at approximately 3400 cm<sup>-1</sup>. The observed vibrations belonging to the ferrocenyl substituent are in agreement with those already reported for similar compounds.<sup>12,14–16</sup>

**Single-Crystal X-ray Diffraction Studies of **2d** and **2f**.** The molecular structures of compounds **2d** and **2f** illustrated in Figures 1 and 2 both contain two molecules per asymmetric unit. Table 1 provides a data collection and refinement summary, and Tables 2 and 3 contain selected bond lengths and angles, and intermolecular bond distances and angles, respectively. The X-ray crystal structures of both compounds show that they belong to the triclinic space group *P* $\bar{1}$  space group and in both *Z* = 4. Each of the structures forms hydrogen-bonded centrosymmetric dimeric units, from symmetry-related monomers. These units link further into infinite chains through additional hydrogen bonding, as shown in Figures 3 and 4; all hydrogen bonds are intermolecular. The pattern of hydrogen bonding is more clearly noted in Scheme 1 for the two compounds. The ladder chains run close to the [001] direction for **2d** and to the [100] direction for **2f**, as illustrated by the corresponding stereodiagrams; hydrogen-bonding parameters for **2d** and **2f** are provided in Table 3. The

(10) (a) Sharma, H.; Cervantes-Lee, F.; Mahmoud, J. S.; Pannell, K. H. *Organometallics* **1999**, *18*, 399. (b) Jakle, F.; Rulkens, R.; Zech, G.; Foucher, D. A.; Lough, A. J.; Manners, I. *Chem. Eur. J.* **1998**, *4*, 2117. (c) Herberhold, M.; Steffl, U.; Milius, W.; Wrackmeyer, B. *Angew. Chem., Int. Ed. Engl.* **1996**, *35*, 1803. (d) Rulkens, R.; Lough, A. J.; Manners, I. *Angew. Chem., Int. Ed. Engl.* **1996**, *35*, 1805. (e) Altmann, R.; Gausset, O.; Horn, D.; Jurkschat, K.; Schürmann, M. *Organometallics* **2000**, *19*, 430. (f) Sharma, H.; Vincenti, S. P.; Vicari, R.; Cervantes-Lee, F.; Pannell, K. H. *Organometallics* **1990**, *9*, 2109.

(11) Foucher, D.; Zieminski, R.; Petersen, R.; Pudelski, M. E.; Ni, Y.; Massey, J.; Jaeger, C. R.; Vancso, J. G.; Manners, I. *Macromolecules* **1994**, *27*, 3992.

(12) MacLachlan, M. J.; Ginzburg, M.; Zheng, J.; Knöll, O.; Lough, A. J.; Manners, I. *New J. Chem.* **1998**, *22*, 1409.

(13) Cella, J. A.; Carpenter, J. C. *J. Organomet. Chem.* **1994**, *480*, 23.

(14) MacLachlan, M. J.; Zheng, J.; Lough, A. J.; Manners, I. *Organometallics* **1999**, *18*, 1337.

(15) MacLachlan, M. J.; Zheng, J.; Thieme, K.; Lough, A. J.; Manners, I.; Mordas, C.; LeSuer, R.; Geiger, W. E.; Liable-Sands, L. M.; Rheingold, A. L. *Polyhedron* **2000**, *19*, 275.

(16) MacLachlan, M. J.; Lough, A. J.; Geiger, W. E.; Manners, I. *Organometallics* **1998**, *17*, 1873.

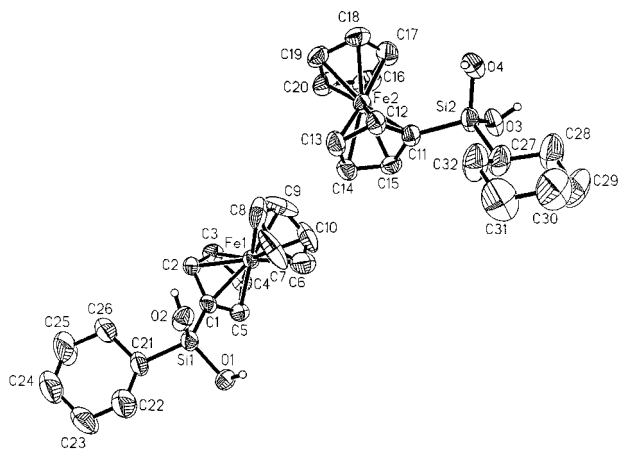


**Figure 2.** Structure and atom-numbering scheme of  $\text{Fc}(\text{cHx})\text{Si}(\text{OH})_2$ ; thermal ellipsoids at 50% probability level.

Si–O bond lengths in **2d** and **2f** range from 1.636 to 1.657 Å, and the O–Si–O angles are in the range 106.1–108.1°, all similar to those reported in previous studies.<sup>22</sup>

Self-assembly in organometallic systems has been recently emphasized,<sup>17</sup> and Scheme 1 illustrates a simplified version of the self-assembled structure for **2d** that can be observed in the stereodiagram presented in Figure 3. Overall the ladder type structure is achieved by linking a pair of dimeric units **A** and **B**, which are in turn held together by a pair of H-bonds. This H-bonding scheme results in an octagonal ring between O3, Si2, H4, and O4 with their centrosymmetric equivalents. There are two distinct crystallographically independent dimeric units within the structure in which either all four of the OH groups are involved in H-bonding (**B**) or only two of them (**A**). Thus in **A** H1 does not participate in hydrogen bonding, resulting in the units **A** and **B** being linked together with a single H-bond. This is in contrast to the related compound  $t\text{-Bu}_2\text{Si}(\text{OH})_2$ , which attains maximum hydrogen bonding.<sup>18</sup> Figure 3 illustrates that the two ferrocenyl molecules are parallel to in each dimeric unit but orthogonal to those in the adjacent dimeric units above and below in the chain.<sup>19</sup>

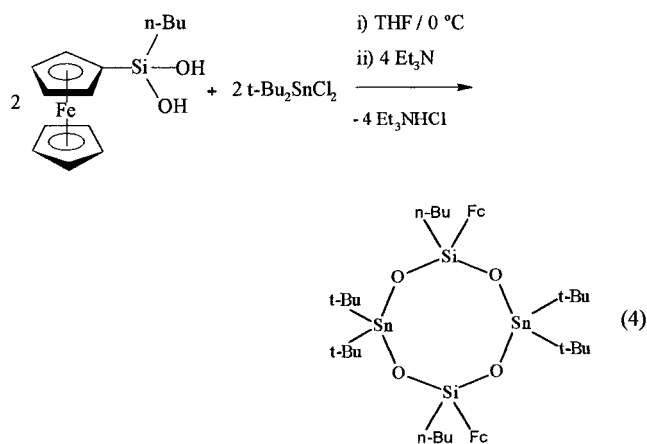
In contrast to **2d**, silanediol **2f** forms a more extensively hydrogen-bonded structure (Figure 4), as has also been observed for  $(\text{c-Hx})_2\text{Si}(\text{OH})_2$ .<sup>20</sup> All the dimeric units are of type **B**, forming two types of crystallographically independent chains. Each chain type consists entirely of symmetry-related monomers. The dimeric units are linked along the ladder chain via two H-bonds. In **2f** the ferrocenyl groups of each dimeric unit are parallel to one another and remain essentially unchanged on the adjacent units. Only one of the two molecules in the asymmetric unit forms one of the observed chains, while

the other chain is comprised solely by the remaining molecule. Both chains differ in orientation with respect to the unit cell of the structure.

Overall the chains observed for **2f** are similar to those described for the related compound  $(\text{cHx})_2\text{Si}(\text{OH})_2$ , while in **2d** a deviation from the structure of  $t\text{-Bu}_2\text{Si}(\text{OH})_2$  is apparent.<sup>18,20</sup> To our knowledge the only other silanol or silanediol structures characterized to date containing a ferrocene moiety, with related self-assembling, are  $\text{Fc}_3\text{-SiOH}$  and diferrocenylsilanediol,  $\text{Fc}_2\text{Si}(\text{OH})_2$ , and the related disiloxanediol  $[\text{HOFc}_2\text{Si}]_2\text{O}$ .<sup>12,14,15</sup>

**Synthesis and Characterization of 3.** There are several reports in the literature concerning the capacity of silanols and stannoxanes to form mixed stannasiloxanes.<sup>9,21</sup> Thus, we have preliminarily evaluated the new silanediols with respect to their capacity to be incorporated into such molecular species.

The reaction between  $\text{Fc}(n\text{-Bu})\text{Si}(\text{OH})_2$  and  $t\text{-Bu}_2\text{-SnCl}_2$  in the presence of triethylamine was carried out at room temperature by slow addition of the chlorostannane to the silanediol/amine mixture in a THF solution, eq 4.



The reaction was monitored by IR spectroscopy. After 15 h no starting material was present, and after filtration, the solvent was removed under vacuum to yield **3** as a yellow solid. The IR spectrum of **3** confirms formation of a stannasiloxane by the presence of a new band at 955  $\text{cm}^{-1}$  that has been attributed to Si–O–Sn vibration.<sup>20</sup> The <sup>13</sup>C, <sup>29</sup>Si, and <sup>119</sup>Sn NMR analysis of the recrystallized material indicates the product to be a mixture of the *cis* and *trans* isomers. The <sup>119</sup>Sn NMR of compound **3**, –158.3 and –158.5 ppm, is in close agreement with those of other eight-membered ring stannasiloxanes with Sn–(O–Si–O)<sub>2</sub>–Sn frameworks (–149.5 to –166.7 ppm).<sup>22</sup> The <sup>29</sup>Si NMR shows two signals of almost equal intensity at –27.08 and –27.14 ppm, considerably downfield from the related chloride (–55.7, –56.0 ppm) and fluoride (–38.9, –39.1 ppm) substituted  $t\text{-Bu}_2\text{Sn}(\text{OSi-}t\text{-Bu(X)O})_2\text{Sn-}t\text{-Bu}_2$  compounds, but close to that of *cyclo*-( $t\text{-Bu}_2\text{SiOSn-}t\text{-Bu}_2\text{O}$ )<sub>2</sub> (–25.7 ppm). Furthermore, the <sup>13</sup>C NMR of **3** exhibits a set of doublets for each of the carbon resonances belonging to the substituted Cp rings, confirming the presence of the *cis/trans* mixture.

Crystals suitable for X-ray analysis were obtained, and the resulting structure is illustrated in Figure 5 and crystallographic parameters and selected bond lengths and angles are provided in Tables 1 and 2. Figure 5a

(17) Haiduc, I.; Edelman, F. T. *Supramolecular Organometallic Chemistry*; Wiley-VCH: New York, 1999.

(18) Buttrus, N. H.; Eaborn, C.; Hitchcock, P. B.; Saxena, A. K. *J. Organomet. Chem.* **1985**, *284*, 291.

(19) Cervantes-Lee, F.; Sharma, H. K.; Pannell, K. H.; Derecskei-Kovacs, A.; Marynick, D. S. *Organometallics* **1998**, *17*, 3701.

(20) Buttrus, N. H.; Eaborn, C.; Hitchcock, P. B.; Lickiss, P. D.; Taylor, A. D. *J. Organomet. Chem.* **1986**, *309*, 25.

(21) Voigt, A.; Murugavel, R.; Ritter, U.; Roesky, H. W. *J. Organomet. Chem.* **1996**, *521*, 279.

(22) Beckmann, J.; Mahieu, B.; Nigge, W.; Schollmeyer, D.; Schürmann, M. *Jurkschat, K. Organometallics* **1998**, *17*, 5697.

Table 1. Crystallographic Data for Compounds 2d, 2f, and 3

	C <sub>14</sub> H <sub>20</sub> FeO <sub>2</sub> Si	C <sub>16</sub> H <sub>22</sub> FeO <sub>2</sub> Si	C <sub>44</sub> H <sub>72</sub> Fe <sub>2</sub> O <sub>4</sub> Si <sub>2</sub> Sn <sub>2</sub>
formula	C <sub>14</sub> H <sub>20</sub> FeO <sub>2</sub> Si	C <sub>16</sub> H <sub>22</sub> FeO <sub>2</sub> Si	C <sub>44</sub> H <sub>72</sub> Fe <sub>2</sub> O <sub>4</sub> Si <sub>2</sub> Sn <sub>2</sub>
color, habit	orange prism	orange prism	orange, irregular fragment
cryst syst	triclinic	triclinic	monoclinic
cryst size, mm	0.32 × 0.44 × 0.80	0.60 × 0.60 × 0.40	0.60 × 0.44 × 0.42
space group	<i>P</i> $\bar{1}$	<i>P</i> $\bar{1}$	<i>C</i> 2/ <i>c</i>
<i>a</i> , Å	10.8470(10)	5.609(2)	25.053(8)
<i>b</i> , Å	10.8770(10)	16.443(6)	9.591(4)
<i>c</i> , Å	13.088(2)	17.035(6)	22.917(8)
$\alpha$ , deg	101.440(10)	87.39(3)	90
$\beta$ , deg	105.240(10)	82.80(3)	115.77(2)
$\gamma$ , deg	91.710(10)	88.29(3)	90
<i>V</i> , Å <sup>3</sup>	1454.8(3)	1556.7(10)	4959(3)
<i>Z</i>	4	4	4
$\rho_{\text{calcd}}$ , mg/m <sup>3</sup>	1.389	1.409	1.434
$\mu$ , mm <sup>-1</sup>	1.107	1.041	1.654
<i>F</i> (000)	640	696	2192
$\theta$ range, deg	3.5–45.0	3.5–45.0	2.31–22.54
index ranges	0 ≤ <i>h</i> ≤ 11 −11 ≤ <i>k</i> ≤ 11 −14 ≤ <i>l</i> ≤ 13	0 ≤ <i>h</i> ≤ 6 −17 ≤ <i>k</i> ≤ 17 −18 ≤ <i>l</i> ≤ 18	−12 ≤ <i>h</i> ≤ 0 −2 ≤ <i>k</i> ≤ 10 −22 ≤ <i>l</i> ≤ 24
no. of reflns collected	4066	4573	3460
no. of ind reflns/ <i>R</i> <sub>int</sub>	3826/0.0211	4072/0.0170	3460/0.0550
no. of obsd reflns with ( <i>I</i> > 2.0 $\sigma$ ( <i>I</i> ))	3428	3386	3226
no. of params	326	362	247
goodness of fit ( <i>F</i> <sup>2</sup> )	1.01	1.55	1.146
<i>R</i> 1( <i>F</i> ) ( <i>I</i> > 2 $\sigma$ ( <i>I</i> ))	0.0420	0.0502	0.0404
w <i>R</i> 2( <i>F</i> <sup>2</sup> ) (all data)	0.0697	0.0682	0.1140
largest diff peak/hole, e/Å <sup>3</sup>	0.44/−0.40	0.76/−0.42	0.601/−0.674

Table 2. Selected Bond Lengths and Angles for Compounds 2d, 2f, and 3<sup>a</sup>

	C <sub>14</sub> H <sub>20</sub> FeO <sub>2</sub> Si	C <sub>16</sub> H <sub>22</sub> FeO <sub>2</sub> Si	
Bond Lengths (Å)			
Si(1)–O(1)	1.648(3)	Si(1)–O(1)	1.657(4)
Si(1)–O(2)	1.636(3)	Si(1)–O(2)	1.639(4)
Si(2)–O(3)	1.650(3)	Si(2)–O(3)	1.645(4)
Si(2)–O(4)	1.618(3)	Si(2)–O(4)	1.642(4)
Si(1)–C(10)	1.838(3)	Si(1)–C(1)	1.848(5)
Si(1)–C(11)	1.858(4)	Si(1)–C(21)	1.860(7)
Si(2)–C(22)	1.859(3)	Si(2)–C(11)	1.834(5)
Si(2)–C(25)	1.678(4)	Si(2)–C(27)	1.870(6)
Bond Angles (deg)			
O(1)–Si(1)–O(2)	108.0(1)	O(1)–Si(1)–O(2)	106.1(2)
O(3)–Si(2)–O(4)	107.3(1)	O(3)–Si(2)–O(4)	108.1(2)
C(10)–Si(1)–C(12)	111.2(2)	C(1)–Si(1)–C(21)	108.4(2)
C(22)–Si(2)–C(25)	114.8(2)	C(11)–Si(2)–C(27)	109.1(3)
C <sub>44</sub> H <sub>72</sub> Fe <sub>2</sub> O <sub>4</sub> Si <sub>2</sub> Sn <sub>2</sub>			
Bond Lengths (Å)			
Sn–O(1)	1.955(4)		
Sn–O(2)	1.957(4)		
Sn–C(15)	2.155(6)		
Sn–C(19)	2.172(6)		
Si(1)–O(1)	1.607(4)		
Si(1)–O(2)	1.604(4)		
Si(1)–C(1)	1.864(6)		
Si(1)–C(11)	1.876(6)		
Bond Angles (deg)			
O(1)–Si(1)–O(2)	111.7(2)		
O(1)–Si(1)–C(1)	110.3(2)		
O(1)–Si(1)–C(11)	106.4(3)		
O(2)–Si(1)–C(1)	106.9(3)		
O(2)–Si(1)–C(11)	109.8(3)		
C(1)–Si(1)–C(11)	111.9(3)		
Si(1)–O(1)–Sn(1)	149.7(3)		
Si(1)–O(2)–Sn(1)	143.9(3)		
C(15)–Sn–C(19)	121.6(2)		

<sup>a</sup> Symmetry transformation used to generate equivalent atoms:  $-x + 1, y, -z + 1/2$ .

shows the molecular structure of **3**, which is a dimer with crystallographic *C*<sub>2</sub> symmetry. Figure 5a also illustrates the *cis* nature with respect to the two ferrocenyl groups. Figure 5b shows the twist conformation adopted by the molecule as well as the tetrahedral

coordination of both Si and Sn atoms. The Sn–O, Sn–C, Si–O, and Si–C bond lengths and the Si–O–Sn bond angles are all comparable to those of reported eight-member stannasiloxanes.<sup>22</sup> The crystal packing of **3** shows all of the ferrocenyl moieties arranged parallel to one another in adjacent molecules, displaying no form of interaction between them. The *cis* isomer isolated in the solid state contrasts with the structure obtained for the related stannasiloxane *t*-Bu<sub>2</sub>Sn[OSi(*t*-Bu)FcO]<sub>2</sub>Sn-*t*-Bu<sub>2</sub>, which was isolated as the *trans* isomer, and this observation illustrates the close energy of these two geometries.

Spectroscopic analysis of the crystals from which the X-ray structure was determined illustrated the immediate presence of both *cis* and *trans* isomers, thereby demonstrating the facile ring-opening and re-formation of the stannasiloxane in solution. This observation has been previously made in related stannasiloxanes, *t*-Bu<sub>2</sub>Sn(OSi-*t*-BuXO)<sub>2</sub>Sn-*t*-Bu<sub>2</sub> (X = F, Cl),<sup>21</sup> and *cyclo*-(Ph<sub>2</sub>-SiOSnR<sub>2</sub>O)<sub>2</sub> R = (CH<sub>2</sub>)<sub>3</sub>NMe<sub>2</sub>.<sup>23</sup>

## Experimental Section

NMR spectra were collected with a Bruker 300 MHz multinuclear spectrometer; IR spectra were acquired with a Perkin-Elmer 1600 FT-IR spectrophotometer in NaCl cells in CH<sub>2</sub>Cl<sub>2</sub> or CCl<sub>4</sub> solvents; UV/vis spectra were recorded with a Lambda 14 Perkin-Elmer spectrophotometer. Melting points were determined in a Mel-Temp II instrument in tubes previously purged with argon and then sealed with a propane torch and are uncorrected. Elemental analyses were performed by Galbraith Laboratories Inc. Chlorosilane compounds were purchased from Gelest; all other chemicals were obtained from Aldrich.

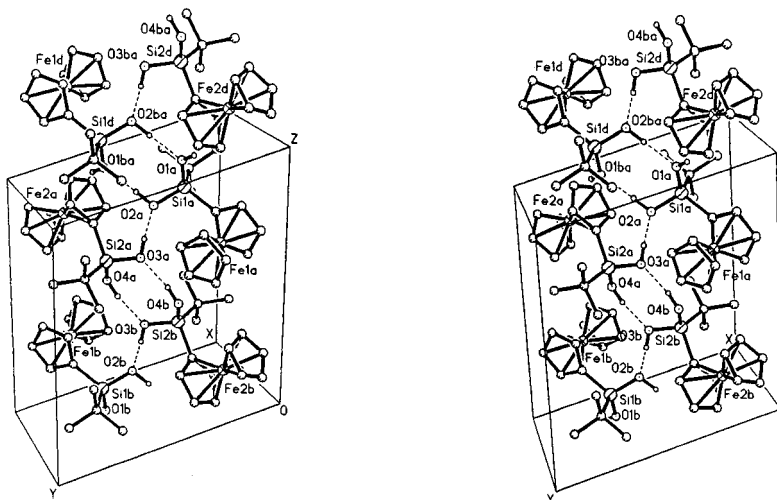
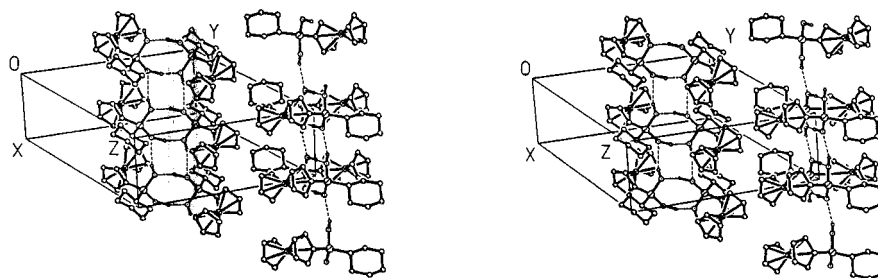
All synthetic manipulations were performed under an inert atmosphere of prepurified dinitrogen or argon, employing standard Schlenk techniques for the handling of air-sensitive

(23) Beckmann, J.; Jurkschat, K.; Kaltenbrunner, U.; Pieper N.; Schürmann, M. *Organometallics* **1999**, *18*, 1586.

**Table 3.** Intermolecular Bond Distances and Angles for Compounds **2d** and **2f**<sup>a</sup>

atoms	distances (Å)		angle (deg)		symmetry	
O4–H4–O3A	O4–H4	0.903	H4–O3A	1.842	168.9	O3A: (-x + 1, -y + 1, -z + 1)
O3–H3–O2	O3–H3	0.981	H3–O2	1.779	176.4	O2: (x, y, z)
O2–H2–O1B	O2–H2	1.000	H2–O1	1.830	176.2	O1B: (-x + 1, -y + 1, -z + 2)
O1–H1–O2B	O1–H1	0.942	H1–O2B	2.191	149.3	O2B: (x + 1, y, z)
O2–H2–O1A	O2–H2	0.955	H2–O1A	1.912	158.2	O1A: (-x + 1, -y, -z)
O3–H3–O4A	O3–H3	1.132	H3–O4A	1.722	162.9	O4A: (-x, -y, -z)
O4–H4–O3C	O4–H4	0.800	H4–O3C	2.358	162.9	O3C: (x - 1, y, z)

<sup>a</sup> H1 is not involved in hydrogen bonding (see stereodiagram).

**Figure 3.** Stereodiagram of  $\text{Fc}(t\text{-Bu})\text{Si}(\text{OH})_2$  showing the hydrogen-bonded chains.**Figure 4.** Stereodiagram of  $\text{Fc}(c\text{-Hx})\text{Si}(\text{OH})_2$  showing the hydrogen-bonded chains along the  $x$ -axis.

reagents. Solvents and reagents were dried prior to use by conventional methods: tetrahydrofuran (THF) was distilled over deep purple sodium/benzophenone ketyl; hexanes over sodium; diethyl ether over lithium aluminum hydride; and triethylamine over sodium. Methyltrichlorosilane ( $\text{MeSiCl}_3$ ) was distilled over anhydrous potassium carbonate and stored over molecular sieves; allyltrichlorosilane ( $\text{CH}_2=\text{CHCH}_2\text{SiCl}_3$ ),  $n$ -butyl trichlorosilane ( $n\text{-BuSiCl}_3$ ), and phenyltrichlorosilane ( $\text{PhSiCl}_3$ ) were distilled and stored over 3 Å molecular sieves, cyclohexyltrichlorosilane ( $c\text{-HxSiCl}_3$ ) was purified by vacuum distillation, and *tert*-butyltrichlorosilane ( $t\text{-BuSiCl}_3$ ) and di-*tert*-butyldichlorostannane ( $t\text{-Bu}_2\text{SnCl}_2$ ) were used as received from Gelest. All glassware joints and stopcocks were fitted with Teflon sleeves to avoid silicone grease contamination.

The ferrocenyldichlorosilanes **1a**, **1b**, **1d**, **1e**, and **1f** were synthesized by the published route for **1a** using ferrocenyllithium and the appropriate  $\text{RSiCl}_3$ ;<sup>24</sup> a typical example is described below.

**Ferrocenyl(2-propenyl)dichlorosilane,  $\text{Fc}(\text{CH}_2=\text{CHCH}_2)\text{SiCl}_2$  (**1b**).** A solution of  $[\text{Fc}]^-\text{Li}^+$  prepared from  $\text{FcHgCl}_2$ <sup>25</sup> (6.3 g, 15.0 mmol) and 19.0 mL of  $n\text{-BuLi}$  in 70 mL of THF was added at  $-78^\circ\text{C}$  to 2.2 mL (15.0 mmol) of a magnetically

stirred solution of  $\text{CH}_2=\text{CHCH}_2\text{SiCl}_3$  in 30 mL of THF. The solution was permitted to warm to ambient temperature and stirred for 15 h. The solvent was removed in vacuo, and the solid residue was extracted with hexanes and filtered through Celite. After removal of  $n\text{-Bu}_2\text{Hg}$ , distillation at  $122\text{--}124^\circ\text{C}/0.2\text{ mmHg}$  yielded  $\text{Fc}(\text{CH}_2\text{CHCH}_2)\text{SiCl}_2$  as a red liquid in 71% yield (3.5 g, 10.8 mmol). NMR ( $\text{CDCl}_3$ ):  $^1\text{H}$  ( $\delta$ , ppm) 2.31 ( $\text{Si}-\text{CH}_2$ ), 4.30 (Fc), 4.39 (Fc), 4.53 (Fc), 5.19 ( $\text{CH}=\text{CH}_2$ ), 5.90 ( $\text{CH}=\text{CH}_2$ );  $^{13}\text{C}$ , 28.80 ( $\text{Si}-\text{CH}_2$ ), 68.19 (Fc), 72.07 (Fc), 73.27 (Fc), 117.40 ( $\text{CH}=\text{CH}_2$ ), 129.54 ( $\text{CH}=\text{CH}_2$ );  $^{29}\text{Si}$ , 18.8.

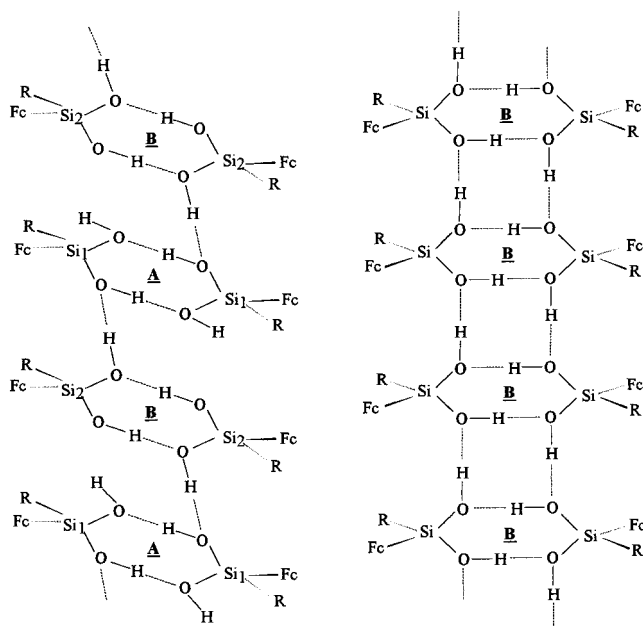
Complexes **1d**, **1e**, and **1f** were prepared in a similar manner, and the various bp's, yields, and NMR spectroscopic data for the new materials are outlined below.

**1d**:  $150\text{--}156^\circ\text{C}/0.2\text{ mmHg}$ , 52% (1.0 g, 2.9 mmol). NMR ( $\text{CDCl}_3$ ):  $^1\text{H}$  ( $\delta$ , ppm) 0.98 ( $\text{CH}_3$ ), 4.15 (Fc);  $^{13}\text{C}$ , 23.5 ( $\text{C}(\text{CH}_3)_3$ ), 24.9 ( $\text{C}(\text{CH}_3)_3$ ), 64.0 (Fc), 69.8 (Fc), 72.4 (Fc), 74.5 (Fc);  $^{29}\text{Si}$ , 30.4.

(24) Foucher, D.; Ziembinski, R.; Petersen, R.; Pudelski, M. E.; Ni, Y.; Massey, J.; Jaeger, C. R.; Vancso, J. G.; Manners, I. *Macromolecules* **1994**, *27*, 3992.

(25) Seyferth, D.; Hofmann, H. P.; Burton, R.; Helling, J. F. *Inorg. Chem.* **1962**, *1*, 227.

**Scheme 1. Self-Assembling Network for 2d (R = *t*-Bu) (left) and 2f (R = *c*-Hx) (right)<sup>a</sup>**



<sup>a</sup> The Si atom numbering for **2d** reflects that illustrated in Figure 3 to permit recognition of the two crystallographically independent dimeric units.

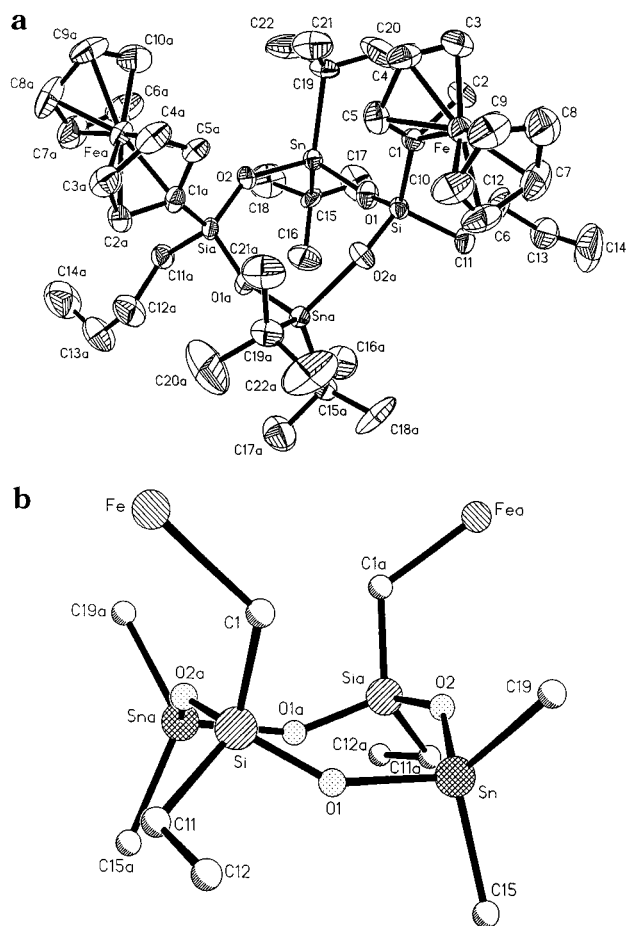


**Figure 5.** (a) Structure and atom-numbering scheme of **3**; thermal ellipsoids at 50% probability level. (b) Plane view showing the twist conformation.

**1e:** 143–146 °C/0.2 mmHg, 58% (1.2 g, 3.3 mmol). NMR (CDCl<sub>3</sub>): <sup>1</sup>H (δ, ppm) 4.30 (5H, Cp), 4.48 (2H, Cp), 4.59 (2H, Cp), 7.50 (Ph), 7.51 (3H, m, Ph *J* = 7.3 Hz), 7.88 (2H, d, Ph *J*

= 7.5 Hz); <sup>13</sup>C, 65.20 (Fc), 69.4 (Fc), 72.3 (Fc), 73.7 (Fc), 128.1 (Ph), 131.3 (Ph), 133.3 (Ph), 133.7 (Ph); <sup>29</sup>Si, 11.0.

**1f:** 197–200 °C/0.2 mmHg, 44% (0.34 g, 1.1 mmol). NMR (CDCl<sub>3</sub>): <sup>1</sup>H (δ, ppm) 1.24–1.88 (*c*-Hx), 4.27 (Fc), 4.32 (Fc), 4.47 (Fc); <sup>13</sup>C, 26.3 (*c*-Hx), 26.5 (*c*-Hx), 27.3 (*c*-Hx), 31.9 (*c*-Hx), 69.7 (Fc), 72.3 (Fc), 74.2 (Fc); <sup>29</sup>Si, 25.7.

Compound **1c** was synthesized by the ring-opening of the corresponding ferrocenophane using a general literature procedure:<sup>14</sup> 96–97 °C/0.15 mmHg. NMR (C<sub>6</sub>D<sub>6</sub>): <sup>1</sup>H (δ, ppm) 0.78, 1.09–1.14, 1.20–1.23, 1.49–1.51 (*n*-Bu); 4.07 (Fc), 4.15 (Fc), 4.19 (Fc), <sup>13</sup>C, 13.73, 22.0, 25.1, 25.7 (*n*-Bu), 66.4 (Fc), 69.6 (Fc), 72.4 (Fc), 73.6 (Fc); <sup>29</sup>Si, 24.5.

**Synthesis of Ferrocenyl(R)silanediols 2a–f.** Hydrolysis of Fc(R)SiCl<sub>2</sub> compounds **1a–f** was performed according to the general synthetic route outlined below specifically for **2a**; similar procedures were used in the preparation of compounds **2b–e**.

**Ferrocenyl(methyl)silanediol, Fc(Me)Si(OH)<sub>2</sub> (2a).** A diethyl ether solution of Fc(Me)SiCl<sub>2</sub> (0.90 g, 3.01 mmol) was slowly added over a period of 1 h to a cooled (0 °C) solution of water (2.1 equiv, 0.12 mL) and Et<sub>3</sub>N (2.0 equiv, 0.84 mL) in 20 mL of ether and 5 mL of acetone (to provide homogeneity). After addition was complete the mixture was further stirred for 40 min while warming to room temperature and concentrated to approximately one-tenth of the original volume. Hexane (~30 mL) was added to promote precipitation, and the resulting mixture was filtered in vacuo to remove the hydrochloride salt. The yellow solution obtained was concentrated in vacuo until one-tenth the volume remained. The mixture was gravity filtered, and the solid product was washed with cold hexanes. The filtrate was concentrated to give a yellow solid that was redissolved in warm hexanes and immediately cooled to 0 °C to precipitate the product. The solid fractions were combined and purified by column chromatography (80–200 mesh silica gel, 20 × 1 cm) with Et<sub>2</sub>O, and the solvent was removed under reduced pressure, providing a pale yellow solid. This material was insoluble in hexane and CCl<sub>4</sub>, moderately soluble in hot CH<sub>2</sub>Cl<sub>2</sub>, CHCl<sub>3</sub>, and C<sub>6</sub>D<sub>6</sub> or CDCl<sub>3</sub>, and completely soluble in Et<sub>2</sub>O, THF, and DMSO; mp 146–147 °C, 79% yield (0.62 g, 2.4 mmol). NMR: <sup>1</sup>H (DMSO-*d*) 0.18 (3H, s, CH<sub>3</sub>), 4.13 (7H, s, η<sup>5</sup>-C<sub>5</sub>H<sub>5</sub> and η<sup>5</sup>-C<sub>5</sub>H<sub>4</sub>), 4.27 (2H, η<sup>5</sup>-C<sub>5</sub>H<sub>4</sub>), <sup>13</sup>C 0.16 (CH<sub>3</sub>), 68.22 (η<sup>5</sup>-C<sub>5</sub>H<sub>5</sub>), 70.19 (η<sup>5</sup>-C<sub>5</sub>H<sub>4</sub>), 70.45 (*ipso*-C), 72.76 (η<sup>5</sup>-C<sub>5</sub>H<sub>4</sub>), <sup>29</sup>Si –16.5. IR (ν, cm<sup>-1</sup>): CH<sub>2</sub>Cl<sub>2</sub>, 3652 (m, sh), 3393 (w, br), 3093 (w), 1423 (w), 1171 (m), 1106 (m), 1037 (m), 1002 (w). UV/vis (λ<sub>max</sub>, nm): CH<sub>2</sub>Cl<sub>2</sub>, 97 (451). Anal. Found (Calcd): C, 49.23 (50.39); H, 5.21 (5.38).

**2b:** mp 94–96 °C, 71% yield (0.66 g, 2.3 mmol). NMR: <sup>1</sup>H 1.87–1.90 (2H, d, Si–CH<sub>2</sub>), 3.84 (2H, br, OH), 4.19 (5H, s, η<sup>5</sup>-C<sub>5</sub>H<sub>5</sub>), 4.25 (2H, t, η<sup>5</sup>-C<sub>5</sub>H<sub>4</sub>), 4.37 (2H, t, η<sup>5</sup>-C<sub>5</sub>H<sub>4</sub>), 4.97–5.08 (2H, m, CH=CH<sub>2</sub>), 5.93–5.96 (1H, m, CH=CH<sub>2</sub>), <sup>13</sup>C 23.55 (Si–CH<sub>2</sub>), 65.57 (*ipso*-C), 68.52 (η<sup>5</sup>-C<sub>5</sub>H<sub>5</sub>), 71.31 (η<sup>5</sup>-C<sub>5</sub>H<sub>4</sub>), 73.15 (η<sup>5</sup>-C<sub>5</sub>H<sub>4</sub>), 114.87 (CH=CH<sub>2</sub>), 133.20 (CH=CH<sub>2</sub>), <sup>29</sup>Si –14.9. IR (ν, cm<sup>-1</sup>): CCl<sub>4</sub>, 3683 (st), 3399 (m, br), 3097 (m), 2975 (w), 1631 (w), 1418 (w), 1172 (st), 1107 (m), 1037 (m), 1002 (w), 901 (m). UV/vis (λ<sub>max</sub>, nm): CH<sub>2</sub>Cl<sub>2</sub>, 114 (450). Anal. Found (Calcd): C, 54.52 (54.18); H, 5.47 (5.60).

**2c:** mp 112–114 °C, 71% yield (1.14 g, 3.7 mmol). NMR: <sup>1</sup>H (CDCl<sub>3</sub>) 0.81–0.92 (5H, m, *n*-Bu), 1.34–1.50 (4H, m, *n*-Bu), 3.18 (2H, br, C), OH), 4.17 (5H, s, η<sup>5</sup>-C<sub>5</sub>H<sub>5</sub>), 4.22 (2H, d, η<sup>5</sup>-C<sub>5</sub>H<sub>4</sub>), 4.36 (2H, d, η<sup>5</sup>-C<sub>5</sub>H<sub>4</sub>), <sup>13</sup>C 13.34 (CH<sub>3</sub>), 14.87 (CH<sub>2</sub>), 24.59 (CH<sub>2</sub>), 25.85 (CH<sub>2</sub>), 66.10 (*ipso*-), 67.98 (η<sup>5</sup>-C<sub>5</sub>H<sub>5</sub>), 70.83 (η<sup>5</sup>-C<sub>5</sub>H<sub>4</sub>), 72.63 (η<sup>5</sup>-C<sub>5</sub>H<sub>4</sub>), <sup>29</sup>Si –9.54. IR (ν, cm<sup>-1</sup>): CCl<sub>4</sub>, 3681 (w, sh), 3346 (w, br), 3094 (w), 2957 (m), 2926 (m), 2871 (w), 1169 (m), 1107 (m), 1036 (m). UV/vis (λ<sub>max</sub>, nm): CH<sub>2</sub>Cl<sub>2</sub>, 93 (445). Anal. Found (Calcd): C, 55.77 (55.27); H, 6.55 (6.62).

**2d:** mp 147–148 °C, 55% yield (0.58 g, 1.9 mmol). NMR: <sup>1</sup>H (CDCl<sub>3</sub>) 0.96 (9H, s, CH<sub>3</sub>), 2.63 (2H, br, OH), 4.20 (5H, s, η<sup>5</sup>-C<sub>5</sub>H<sub>5</sub>), 4.22 (2H, t, η<sup>5</sup>-C<sub>5</sub>H<sub>4</sub>), 4.38 (2H, t, η<sup>5</sup>-C<sub>5</sub>H<sub>4</sub>), <sup>13</sup>C 18.10 (C(CH<sub>3</sub>)<sub>3</sub>), 25.74 (C(CH<sub>3</sub>)<sub>3</sub>), 64.47 (*ipso*-C), 68.30 (η<sup>5</sup>-C<sub>5</sub>H<sub>5</sub>), 71.34 (η<sup>5</sup>-C<sub>5</sub>H<sub>4</sub>), 73.69 (η<sup>5</sup>-C<sub>5</sub>H<sub>4</sub>), <sup>29</sup>Si –9.80. IR (ν, cm<sup>-1</sup>): CCl<sub>4</sub>, 3683 (m, sh), 3644 (w), 3395 (w, br), 3097 (w), 2954 (st), 2932

(st), 2892 (m), 2857 (m), 1473 (m), 1463 (w), 1422 (w), 1391 (w), 1362 (w), 1169 (st), 1107 (m), 1036 (m), 1004 (m). UV/vis ( $\lambda_{\text{max}}$ , nm): CH<sub>2</sub>Cl<sub>2</sub>, 117 (450). Anal. Found (Calcd): C, 54.83 (55.27); H, 6.34 (6.63).

**2e**: mp 140–142 °C, 73% yield (0.33 g, 1.0 mmol). NMR: <sup>1</sup>H (CDCl<sub>3</sub>) 3.21 (2H, br, OH), 4.10 (5H, s,  $\eta^5$ -C<sub>5</sub>H<sub>5</sub>), 4.24 (2H, d,  $\eta^5$ -C<sub>5</sub>H<sub>4</sub>), 4.37 (2H, d,  $\eta^5$ -C<sub>5</sub>H<sub>4</sub>), 7.38–7.43 (3H, m, Ph), 7.72–7.75 (2H, m, Ph), <sup>13</sup>C 65.30 (ipso-C), 68.58 ( $\eta^5$ -C<sub>5</sub>H<sub>5</sub>), 71.59 ( $\eta^5$ -C<sub>5</sub>H<sub>4</sub>), 73.54 ( $\eta^5$ -C<sub>5</sub>H<sub>4</sub>), 127.90 (Ph), 130.27 (Ph), 133.91 (Ph), 135.39 (Ph), <sup>29</sup>Si –8.15. IR ( $\nu$ , cm<sup>-1</sup>): CCl<sub>4</sub>, 3652 (m, sh), 3427 (w, br), 3070 (w), 3040 (w), 1429 (m), 1171 (st), 1036 (m), 904 (w). UV/vis ( $\lambda_{\text{max}}$ , nm): CH<sub>2</sub>Cl<sub>2</sub>, 116 (451). Anal. Found (Calcd) C, 58.76 (59.27); H, 5.02 (4.97).

**2f**: mp 144–147 °C, 72% yield (0.54 g, 1.6 mmol). NMR: <sup>1</sup>H (CDCl<sub>3</sub>) 1.23–1.80 (10H, m, *c*-Hx), 2.61 (2H, br, OH), 4.19 (5H, s,  $\eta^5$ -C<sub>5</sub>H<sub>5</sub>), 4.21 (2H, s,  $\eta^5$ -C<sub>5</sub>H<sub>4</sub>), 4.37 (2H, s,  $\eta^5$ -C<sub>5</sub>H<sub>4</sub>), <sup>13</sup>C 26.06 (CH<sub>2</sub>), 26.64 (CH<sub>2</sub>), 26.69 (CH<sub>2</sub>), 27.60 (CH<sub>2</sub>), 65.64 (ipso-C), 68.33 ( $\eta^5$ -C<sub>5</sub>H<sub>5</sub>), 71.29 ( $\eta^5$ -C<sub>5</sub>H<sub>4</sub>), 73.38 ( $\eta^5$ -C<sub>5</sub>H<sub>4</sub>), <sup>29</sup>Si –11.7. IR ( $\nu$ , cm<sup>-1</sup>): CCl<sub>4</sub>, 3683 (m, sh), 3376 (w, br), 3098 (w), 2923 (st), 2849 (s), 1447 (m), 1261 (w), 1170 (m), 1106 (s), 1036 (st). UV/vis ( $\lambda_{\text{max}}$ , nm): CH<sub>2</sub>Cl<sub>2</sub>, 110 (455). Anal. Found (Calcd): C, 58.01 (58.19); H, 6.71 (6.71).

**Synthesis of 1,1,5,5-Tetra-*tert*-butyl-3,7-*n*-butyl-3,7-ferrocenyl-2,4,6,8-tetraoxa-3,7-disila-1,5-distannacyclooctane, *t*-Bu<sub>2</sub>Sn(OSi(*n*-Bu)FcO)<sub>2</sub>Sn-*t*-Bu<sub>2</sub> (**3**)**. To a 10 mL THF solution of Fc(*n*-Bu)Si(OH)<sub>2</sub> (0.089 g, 0.29 mmol) and Et<sub>3</sub>N (4 equiv, 0.16 mL) maintained at room temperature under an argon atmosphere was added slowly via syringe 10 mL of a THF solution of di-*tert*-butyltindichloride (0.089 g, 0.29 mmol). The solution became turbid after addition of the tin halide and was stirred overnight. The mixture was concentrated under vacuum and filtered through Celite, and the solids were dissolved in hexanes followed by filtration to remove the hydrochloride salt. Evaporation of the yellow solution yielded a crystalline powder. X-ray quality crystals were obtained from the slow evaporation of a hexane solution at room temperature; mp 204–206 °C, 61% yield (0.54 g, 0.5 mmol). NMR: <sup>1</sup>H (CDCl<sub>3</sub>) 0.93, 1.11, 1.24, 1.35, 1.54 (unresolved), 4.08 (2H, s,  $\eta^5$ -C<sub>5</sub>H<sub>5</sub>), 4.10 (2H, s,  $\eta^5$ -C<sub>5</sub>H<sub>5</sub>), 4.14 (1H, d,  $\eta^5$ -C<sub>5</sub>H<sub>5</sub>), 4.17 (2H, m,  $\eta^5$ -C<sub>5</sub>H<sub>4</sub>), 4.20 (2H, m,  $\eta^5$ -C<sub>5</sub>H<sub>5</sub>), <sup>13</sup>C 13.98 (CH<sub>3</sub>), 19.39 (CH<sub>2</sub>, d, *J* = 15 Hz), 26.92 (CH<sub>2</sub>, t, *J* = 4 Hz), 29.66 (SnCMe<sub>3</sub>, t, *J* = 11 Hz), 37.76 (Sn-C, t, *J* = 19 Hz), 46.05 (CH<sub>2</sub>), 68.28 ( $\eta^5$ -C<sub>5</sub>H<sub>5</sub>), 69.80 and 69.84 ( $\eta^5$ -C<sub>5</sub>H<sub>4</sub>), 73.65 and 73.70 ( $\eta^5$ -C<sub>5</sub>H<sub>4</sub>), 74.53 (ipso-C), –27.08, <sup>29</sup>Si –27.14, <sup>119</sup>Sn –158.3, –158.5. IR ( $\nu$ , cm<sup>-1</sup>): CCl<sub>4</sub>, 3098 (w), 2956 (st), 2924

(st), 2871 (m), 2852 (st), 1467 (m), 1413 (w), 1368 (m), 1297 (w), 1261 (w), 1194 (w), 1165 (st), 1107 (m), 1079 (m), 1035 (st), 1004 (st), 955 (m), 893 (w), 818 (w), 688 (w). UV/vis ( $\lambda_{\text{max}}$ , nm): Hex, 178 (440). Anal. Found (Calcd): C, 49.50 (49.30); H, 6.84 (6.78).

**Crystal Structure Determination.** Three orange crystals of approximate dimensions 0.32 × 0.44 × 0.80 mm (**2d**), 0.60 × 0.60 × 0.40 mm (**2f**), and 0.42 × 0.44 × 0.60 mm (**3**) were mounted on glass fibers in a random orientation. Intensity data were collected at room temperature for all compounds using a Siemens/Bruker four-circle diffractometer with graphite-monochromated Mo K $\alpha$  radiation;  $\lambda$  = 0.71073 Å. Unit cell parameters and standard deviations were obtained by least-squares fit of 25 reflections randomly distributed in reciprocal space in the  $2\theta$  range of 15–30°. The  $\omega$ -scan technique was used for intensity measurements in all cases. A range of 1.4° in  $\omega$  and variable speed of 3.00–15.00 deg/min was used for **2d** and a 1.2° in  $\omega$ -range, a 4.00–20.00 deg/min speed for **2f**, whereas for **3** the range was 1.5° in  $\omega$  and the scanning variable speed 4.00–20.00 deg/min. Background counts were taken with a stationary crystal and a total background time to scan time ratio of 0.5. Three standard reflections were monitored in all cases every 97 reflections and showed no significant decay for each crystal. The data were corrected for Lorentz and polarization effects, and a semiempirical absorption correction was also applied to both data sets, giving a min./max. transmission ratio of 0.387/0.431 for **2d** and 0.513/0.618 for **2f**. No absorption correction was applied in the case of **3**. All structures were solved by direct methods and refined using the PC-version of the SHELEXTL PLUS crystallographic software by Siemens. Full-matrix least-squares refinement minimizing  $\sum w(F_o - F_c)^2$  was carried out with anisotropic thermal parameters for non-hydrogen atoms. Hydrogen atoms not attached to oxygen were placed at calculated positions (C–H = 0.96 Å; U<sub>H</sub> = 0.08) during refinements, and those for the hydroxy groups were located on a difference map. The weighing scheme has the form  $w^{-1} = \sigma^2(F) + gF^2$ , and the final *R* factors the form  $R = \sum |F_o - F_c| / \sum F_o$  and  $R_w = [\sum w(F_o - F_c)^2 / \sum wF_o^2]^{1/2}$ .

**Acknowledgment.** This research was supported by the Welch Foundation, Grant AH-0546.

OM010378L